J Supercond Nov Magn
DOI 10.1007/s10948-016-3377-6

ORIGINAL PAPER

Electronic Structure of NaFeAs Superconductor: LDA+DMFT Calculations Compared with ARPES Experiment

I. A. Nekrasov[1] · N. S. Pavlov[1] · M. V. Sadovskii[1,2]

Received: 29 November 2015 / Accepted: 11 December 2015

Abstract In this work, we present a theoretical explanation of the recent high quality angle-resolved photoemission (ARPES) experiments on a new iron-pnictide high temperature superconductor NaFeAs (Evtushinsky arXiv:1409.1537). Well known and rather universal manifestation of correlation effects in iron-pnictides is the renormalization of conducting bands near the Fermi level. Most suitable theoretical technique to describe this effect is LDA+DMFT. Our LDA+DMFT calculations demonstrate that for NaFeAs the mass renormalization by the factor of the order of 3, in good agreement with ARPES experiments, can be achieved, taking into account only correlations on Fe-3d orbitals. No additional interactions with "bosonic" modes, as proposed in Evtushinsky (arXiv:1409.1537), are necessary to describe the experimental data.

Keywords High-temperature superconductors · Iron Pnictides · Dynamical mean-field theory

The family of iron-based high-temperature superconductors first discovered in 2008 [2] still attracts a lot of scientific attention. Experimental and theoretical works on these materials are now discussed in several extended reviews [3–7]. Detailed comparison of electronic band structures of iron pnictides and iron halcogenides, together with some related compounds, was given in Refs. [8, 9].

One of the classes of iron pnictides is the so called 111 system with parent compound $Li_{1-x}FeAs$ with $T_c = 18$ K [10, 11]. LDA band structure of the LiFeAs was first described in the Refs. [12, 13].

One of the most effective experimental techniques to probe electronic band structure of these and similar systems is the angle-resolved photoemission spectroscopy (ARPES) [14]. A review of the present day status of ARPES results for iron-based superconductors can be found in Ref. [15, 16].

Soon after the discovery of iron-based superconductors, it was shown both experimentally [17–21] (mainly by ARPES) and theoretically [22–25] (within the LDA+DMFT hybrid computational scheme [26, 27]) that electronic correlations on Fe sites are essential to describe the physics in these materials. The main manifestation of correlations is simple narrowing (compression) of LDA bandwidth near the Fermi level by the factor of the order from 2 to 4. At the same time, the topology of ARPES determined Fermi surfaces is quite similar to those obtained from simple LDA calculations, showing two or three hole cylinders around Γ–point in the Brillouin zone and two electron Fermi surface sheets around (π, π) point.

This work was inspired by recent high quality ARPES data for NaFeAs system [1] and is devoted to the detailed comparison of these results with LDA+DMFT calculations of electronic structure of this system, showing rather satisfactory agreement with these experiments. Thus, only the account of electronic correlations is sufficient to explain the major features of electronic spectrum of NaFeAs, and there is no need for any additional interactions with any kind of Boson modes (as was suggested in Ref. [1]).

The crystal structure of NaFeAs has tetragonal structure with the space group $P4/nmm$ and lattice parameters

✉ I. A. Nekrasov
nekrasov@iep.uran.ru

[1] Institute for Electrophysics, Russian Academy of Sciences, Ural Branch, Amundsen str. 106, Ekaterinburg 620016, Russia

[2] M.N. Mikheev Institute for Metal Physics, Russian Academy of Sciences, Ural Branch, S.Kovalevskoi str. 18, Ekaterinburg 620290, Russia

Published online: 03 February 2016

$a = 3.9494$ Å, $c = 7.0396$ Å. The experimentally obtained crystallographic positions are the following Fe(2b) (0.75, 0.25, 0.0), Na(2c) (0.25, 0.25, z_{Na}), As(2c) (0.25, 0.25, z_{As}), $z_{As} = 0.20278$, $z_{Na} = 0.64602$ [28]. That is quite similar to LiFeAs crystal structure [10, 12].

In Fig. 1, we show LDA band dispersions near the Fermi level at the plane with $k_z = 0$ calculated within FP-LAPW method [29]. Bands in the vicinity of the Fermi level have predominantly Fe-3d character and are essentially similar to the previously studied case of LiFeAs described elsewhere [12, 13]. In more details, band structure of NaFeAs is reported in the Ref. [30].

To perform DMFT part of LDA+DMFT calculations, we used CT-QMC impurity solver [33–38]. In order to link LDA and DMFT, we exploited Fe-3d and As-4p projected Wannier functions LDA Hamiltonian for about 1500 k-points. Standard wien2wannier interface [31] and wannier90 projecting technique [32] were applied to this end. The DMFT(CT-QMC) computations were done at reciprocal temperature $\beta = 40$ with about 10^7 Monte-Carlo sweeps. Hubbard model interaction parameters were taken to be $U = 3.5$ eV and $J = 0.85$ eV as typical values for pnictides in general and close NaFeAs relative–LiFeAs in particular [39–41].

To produce LDA+DMFT spectral function maps for direct comparison with ARPES data, we need to know the local self-energy $\Sigma(\omega)$. To find it, we have to perform analytic continuation from Matsubara frequencies to real ones. To this end, we have applied Pade approximant algorithm [42] (for details see Ref. [30]). Corresponding self-energies for different Fe-3d orbitals near the Fermi level are shown on Fig. 2. From the real part of self-energy, we can obtain the mass renormalization factor for different orbitals: $m^*/m_{xy} \approx 3.8$, $m^*/m_{xz,yz} \approx 3.9$, $m^*/m_{3z^2-r^2} \approx 2$, and $m^*/m_{x^2-y^2} \approx 1$. These numbers agree well with variety of the previous theoretical works for LiFeAs and NaFeAs [39–41]. Thus, only the account of local Coulomb correlations on the Fe sites is enough to produce such renormalization and no extra interaction with possible Boson mode is necessary in contrast to the proposal of Ref. [1].

Typically, experimental ARPES data are presented in a rather narrow energy interval of few tenth of electronvolt close to the Fermi level (for LiFeAs and NaFeAs see Refs. [41, 43–46]). However, in Ref. [1] ARPES, data were measured down to a quite large binding energies about 6 eV with rather high resolution allowing to extract different bands.

In Fig. 3, we compare experimental ARPES spectral functions for NaFeAs (left panel) [1] along the MΓM high symmetry direction with LDA+DMFT calculated (middle panel) spectral function map for a wide energy window. On both of these panels, one can see rather high intensity region from 0 to 0.5 eV formed by quasiparticle bands near the Fermi level, and then from −2 to −5 eV, we can observe As-4p bands. To compare experimental and theoretical band dispersions on the right panel of Fig. 3, we plot the dispersions for the maxima of experimental (crosses) and theoretical (white lines) spectral functions.

According to Ref. [1], ARPES bands line shapes remind very much the LDA bands, compressed by an almost constant factor of the order of 3 for all energies. By analyzing the real part of self-energies from Fig. 2, we can convince ourselves that this correlation narrowing is essentially frequency dependent. Extended discussion of similar situation was given in our recent work on $KaFe_2Se_2$ [49, 50]. Actually, the LDA bands located in the interval from −0.5 to 0.25 eV become more narrowed due to correlations. At larger energies, the bands stay at about the same positions as in LDA or get more spread in energy since the slope of the real part of self-energy is changed to the positive one.

As to As-4p bands, ARPES experiment resolves only two bands instead of six (2 As atoms in the unit cell). Despite the general shape of the bands being quite similar in both cases, the experiment shows As-4p states about 0.5 eV lower in energy than obtained in LDA+DMFT.

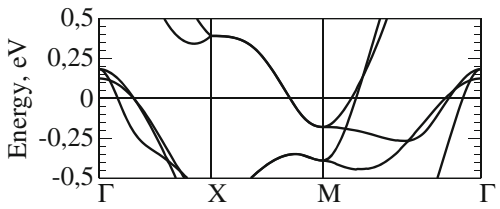

Fig. 1 LDA calculated band dispersions of paramagnetic NaFeAs near the Fermi level for $k_z = 0$ high symmetry directions. The Fermi level E_F is at zero energy

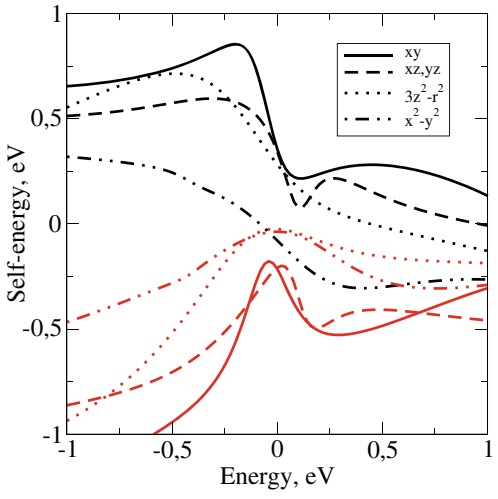

Fig. 2 LDA+DMFT calculated self-energies for different Fe-3d orbitals of NaFeAs near the Fermi level. *Black lines* indicate real part and *gray lines* indicate imaginary part. The Fermi level E_F is at zero energy

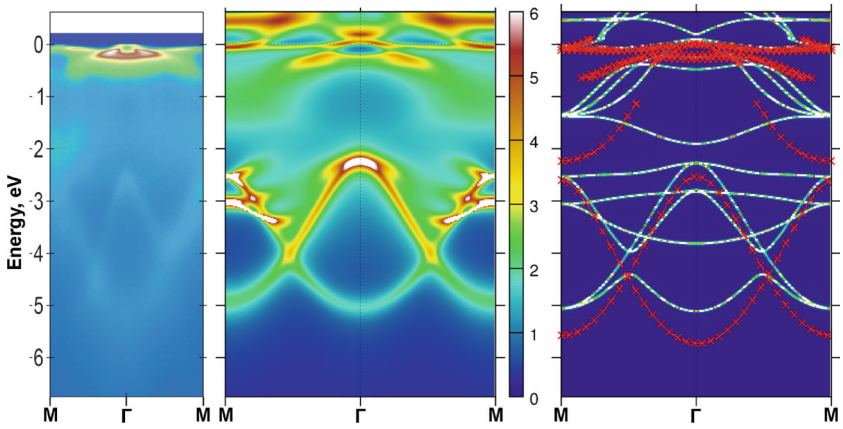

Fig. 3 Comparison of experimental ARPES (*left panel*) [1] and LDA+DMFT (*middle panel*) spectral functions in the MΓM high symmetry direction for NaFeAs for the wide range of binding energies containing Fe-3d and As-4p states. On the *right panel*, maxima of experimental (*crosses*) [1] and theoretical (*white lines*) extracted from corresponding spectral functions are presented. The Fermi level E_F is at zero energy

This can be explained in the framework of generalized LDA'+DMFT calculations [47, 48], which allows one a better description of Fe(3d)-As(4p) energy splitting, as was shown for example for $KaFe_2Se_2$ system [49, 50]. Indeed, our LDA'+DMFT calculations showed that As-4p states appeared about 0.5 eV lower in energy.

Between quasiparticle bands and As-4p bands, there is a rather low intensity region (−0.5−−2 eV) seen in Fig. 3 on the left and middle panels. First of all, it appears because there are almost no bands in this energy interval, and second, in this region, we have a crossover from the well-defined quasiparticle bands with quite low damping to the rest of the bands placed at higher binding energies. This fact is illustrated by gray lines in Fig. 2, representing the imaginary parts $\Sigma''(\omega)$ of LDA+DMFT calculated self-energies for all Fe-3d orbitals. Near energy zero (Fermi level) $\Sigma''(\omega)$ is about 0.2 eV or less for all correlated states. At the same time, real parts of the self-energies $\Sigma'(\omega)$ have negative slope near the Fermi level, which corresponds to well-defined quasiparticles. Following $\Sigma'(\omega)$ behavior, one can find that it has peak at about 0.25 eV, which corresponds to the end of quasiparticle region and $\Sigma''(\omega)$ grows quite rapidly beyond this energy. Nearly, the same behavior of $\Sigma'(\omega)$ and $\Sigma''(\omega)$ was assumed in the Ref. [1] and related to interaction with some "unknown Boson mode", distinguishing NaFeAs as unconventional superconductor. Again, we claim that just the local Coulomb correlations on the Fe sites can do all that alone.

Now, we turn to the quasiparticle bands dispersions in the close proximity if the Fermi level. Corresponding comparison of experimental ARPES data and theoretical LDA+DMFT spectral functions for NaFeAs is given in Fig. 5. Here, we show only the data for MΓM high symmetry direction, the results for other symmetry directions can be found in the Ref. [30]. Experimental data were obtained at two different rather distinctive beam energies around 80 and 160 eV (see panels c and d in Fig. 4). At bird eye view for both beam energies, experimental picture looks similar, but in fact there are some remarkable differences. For 84 eV data, xy and xz, yz bands close to the Fermi level are more intensive as compared to 160 eV data. On the other hand, $3z^2 - r^2$ band at about −0.2 eV looks more intensive in 160 eV data.

To clarify this fact, we suggest the following explanation. It is well known that by varying the beam energy in ARPES experiments one can access different values of k_z component of the momenta [14]. However, to get the precise value of k_z, one should know the exact geometry of ARPES

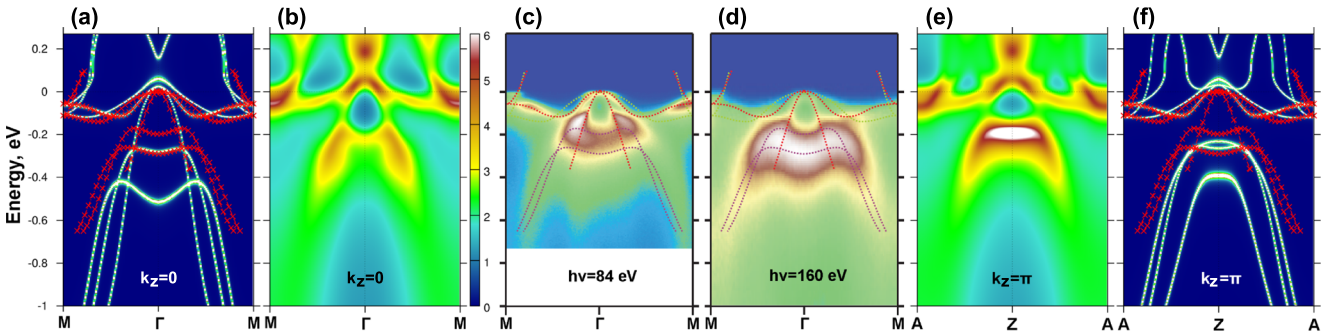

Fig. 4 Comparison of experimental ARPES (panels **c** and **d**) [1] and LDA+DMFT (panels **b** and **e**) spectral functions in the MΓM and AZA high symmetry directions for NaFeAs near the Fermi level. On the panels **a** and **f**, experimental (*crosses*) [1] and theoretical (*white lines*) maxima dispersions of spectral functions are presented. The Fermi level E_F is at zero energy

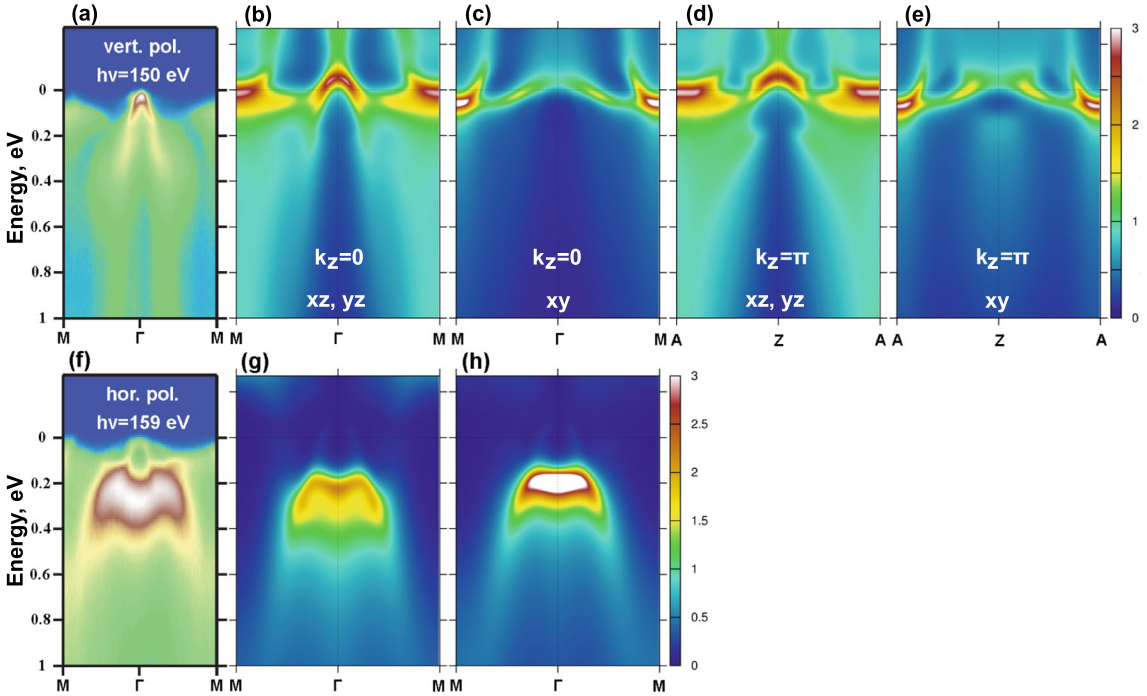

Fig. 5 Comparison of experimental ARPES spectral functions with different polarization (panel **a** indicates vertical polarization and panel **f** indicates horizontal polarization) [1] and LDA+DMFT spectral functions for different Fe-3d orbitals: panels **b**–**e** indicate xz, yz and xy contributions, panels **g** and **h** indicate $3z^2 - r^2$ contribution in the MΓM high symmetry direction for NaFeAs near the Fermi level for $k_z = 0$ and $k_z = \pi$ cases. The Fermi level E_F is at zero energy

experiment [14], work function and inner potential for this particular material [51]. Since we do not know all these precisely, we can try some speculations. In Fig. 4, we plotted LDA+DMFT calculated spectral functions for $k_z = 0$ (panel b) and $k_z = \pi$ (panel e). Now moving from $k_z = 0$ (panel b) to $k_z = \pi$ (panel e), we can observe the same trend as one goes from 84 eV (panel c) to 160 eV (panel d) beam energy in the experiment.

Although iron-based superconductors have pronounced layered structure still these systems are *quasi* two-dimensional and thereby possess some finite dispersion along k_z axis. This fact is reflected on panels a and f of Fig. 4 where LDA+DMFT spectral function maxima dispersions (white lines) are shown at $k_z = 0$ (panel a) and $k_z = \pi$ (panel f). For the case of $k_z = \pi$ (panel f) xz, yz bands are no more degenerate in Γ-point. One of xz, yz band branches goes down in energy to -0.2 eV and becomes degenerate with one of $3z^2 - r^2$ bands. At the same time, $3z^2 - r^2$ band goes down to -0.4 eV at Γ-point and becomes more flat. All that, in contrast to the $k_z = 0$ case, results in higher intensity of LDA+DMFT spectral function (panel e) around -0.2 eV and lower intensity at the Fermi level. The later one agrees better with 160 eV ARPES data, than with 84 eV ARPES data. Here, one should stress that xy band and one

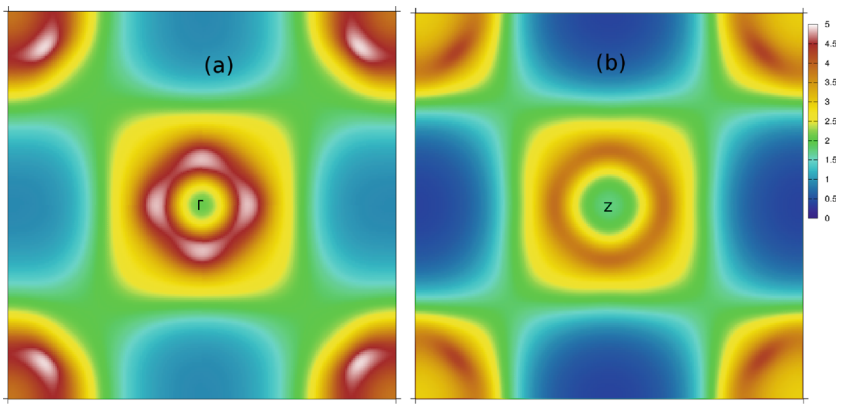

Fig. 6 LDA+DMFT calculated Fermi surface maps for NaFeAs. Panel **a** indicates $k_z = 0$ and **b** indicate $k_z = \pi$

of xz, yz bands branches right below the Fermi level keep their shapes almost unchanged for both $k_z = 0$ and $k_z = \pi$.

Somewhat larger intensity of LDA+DMFT spectral functions in comparison with experiment near M point arises because of quite strong xy contribution in this region. However, in the ARPES data [1], xy band is almost hidden, perhaps due to matrix elements effects. Note also that shown experimental ARPES maxima (crosses on panels a and f) in accordance with Ref. [1] do not depend on beam energy.

To discuss different Fe-3d orbitals contribution to spectral function maps, we used experimental ARPES spectral functions obtained for different polarizations [1]. In Fig. 5, panel a corresponds to vertical polarization ARPES data in the MΓM high symmetry direction taken at 160 eV and panel f corresponds to the horizontal polarization. For vertically polarized beam, "cap"-like structure around Γ-point is formed mainly by xz, yz orbitals (panels b and d for LDA+DMFT results). Surprisingly, the intensity of xy band (panels c and e) is quite low in ARPES data and even not addressed in Ref. [1]. The k_z dispersion of these bands near the Fermi level is almost absent. Horizontally polarized beam (panel f) wipes out $3z^2 - r^2$ band forming "M"-like structure around -0.2 eV. For $k_z = \pi$, it has higher intensity than for $k_z = 0$. It is in better agreement with to 159 eV data.

In Fig. 6, there are drawn isoenergetic spectral function maps for $k_z = 0$ (panel a, Fermi surface, and $k_z = \pi$ on panel b). On both panels, we see rather broadened Fermi surface sheets around Γ and M R points (panel a) and Z and R points (panel b). Also, both pictures are quite similar. That fact reflects quasi two-dimensional nature of the NaFeAs band structure. Although on panel (a) map i somewhat more intensive.

In this paper, we have presented the results of extended LDA+DMFT(CT-QMC) theoretical analysis of recent high quality angle-resolved photoemission (ARPES) experiments on a new iron-pnictide high temperature superconductor NaFeAs [1]. The well known and rather universal manifestation of correlation effects in iron-pnictides is the renormalization (narrowing) of conducting bands near the Fermi level by a factor of 2 to 4. Corresponding mass renormalization factors for different orbitals were obtained from LDA+DMFT calculations and, in our opinion, no extra interaction with some "unknown Boson mode" distinguishing NaFeAs as unconventional superconductor is necessary in contrast to the suggestion of Ref. [1].

Also, we have shown that ARPES data taken at 160 eV beam energy most probably corresponds to $k_z = \pi$ Brillouin zone boundary, while the data measured at about 80 eV beam energy reproduces $k_z = 0$. Theoretical analysis of spectral weight redistribution support this point of view. Comparison of different Fe-3d orbitals contributions to spectral function maps for vertically and horizontally polarized ARPES data also favors the last statement.

Acknowledgments We thank D. Evtushinsky for many helpful discussions of the ARPES experimental data, A. Lichtenstein and I. Krivenko for providing us their CT-QMC code, and A. Sandvik for making available his maximum entropy program. We are especially grateful to G.N. Rykovanov for providing us the access to VNIITF "Zubr" supercomputer, at which most of our CT-QMC computations were performed. Also, part of CT-QMC computations were performed at supercomputer "Uran" at the Institute of Mathematics and Mechanics UB RAS.

This work was done under the State Contract No. 0389-2014-0001 and partly supported by RFBR grant No. 14-02-00065.

References

1. Evtushinsky, D.V., et al.: arXiv:1409.1537
2. Kamihara, Y., Watanabe, T., Hirano, M., Hosono, H.: J. Am. Chem. Soc. **130**, 3296–3297 (2008)
3. Sadovskii, M.V.: Uspekhi Fiz. Nauk **178**, 1243 (2008)
4. Sadovskii, M.V.: Physics Uspekhi **51**(12) (2008)
5. Ishida, K., Nakai, Y., Hosono, H.: J. Phys. Soc. Jpn. **78**, 062001 (2009)
6. Johnson, D.C.: Adv. Phys. **59**, 803 (2010)
7. Hirshfeld, P.J., Korshunov, M.M., Mazin, I.I.: Rep. Prog. Phys. **74**, 124508 (2011)
8. Sadovskii, M.V., Kuchinskii, E.Z., Nekrasov, I.A.: JMMM **324**, 3481 (2012)
9. Nekrasov, I.A., Sadovskii, M.V.: Pis'ma Zh. Eksp. Teor. Fiz. **99**, 687 (2014). [JETP Letters, 99, 598 (2014)]
10. Tapp, J.H., et al.: Phys. Rev. B **78**, 060505(R) (2008)
11. Wang, X.C., et al.: Solid State Commun. **11-12**, 538 (2008)
12. Nekrasov, I.A., Pchelkina, Z.V., Sadovskii, M.V.: Pis'ma Zh. Eksp. Teor. Fiz. **88**, 621 (2008). [JETP Letters **88**, 543]
13. Shein, I.R., Ivanovskii, A.L.: Pis'ma Zh. Eksp. Teor. Fiz. **88**, 377 (2008). [JETP Letters, **88**, 329 (2008)]
14. Damascelli, A., Hussain, Z., Shen, Z.-X.: Rev. Mod. Phys. **75**, 473 (2003)
15. Kordyuk, A.A.: Fizika Nizkikh Temperatur **38**, 1119 (2012)
16. Kordyuk, A.A.: Low Temp. Phys. **38**, 888 (2012)
17. Popovich, P., et al.: Phys. Rev. Lett. **105**, 027003 (2010)
18. Borisenko, S., et al.: Phys. Rev. Lett. **105**, 067002 (2010)
19. Ding, H., et al.: J. Phys. Condens. Matter **23**, 135701 (2011)
20. Cui, S.T., et al.: Phys. Rev. B **86**, 155143 (2012)
21. Evtushinsky, D.V., et al.: Phys. Rev. B **89**, 064514 (2014)
22. Haule, K., Shim, J.H., Kotliar, G.: Phys. Rev. Lett. **100**, 226402 (2008)
23. Craco, L., et al.: Phys. Rev. B **78**, 134511 (2008)
24. Shorikov, A.O., et al.: Zh. Eksp. Teor. Fiz. **135**, 134 (2009). [JETP **108**, 121 (2008)]
25. Skornyakov, S.L., et al.: Phys. Rev. B **80**, 092501 (2009)
26. Held, K., et al.: Int. J. Mod. Phys. B **15**, 2611 (2001)
27. Kotliar, G., et al.: Rev. Mod. Phys. **78**, 865 (2006)
28. Parker, D.R., et al.: Chem. Commun. **16**, 2189 (2009)
29. Blaha, P., et al.: An Augmented Plane Wave + Local Orbitals Program for Calculating Crystal Properties (Techn. Universitat Wien, Austria), 2001. ISBN 3-9501031-1-2
30. Nekrasov, I.A., Pavlov, N.S., Sadovskii, M.V.: Pisma v ZhETF **102**, 30 (2015). [JETP Letters 102, 26 (2015)]. arXiv:1505.04963
31. Kunes, J., et al.: Comp. Phys. Commun. **181**, 1888 (2010)

32. Mostofi, A.A., Yates, J.R., Lee, Y.-S., Souza, I., Vanderbilt, D., Marzari, N.: Comput. Phys. Commun. **178**, 685 (2008)
33. Werner, P., et al.: Phys. Rev. Lett. **97**, 076405 (2006)
34. Haule, K.: Phys. Rev. B **75**, 155113 (2007)
35. Gull, E., et al.: Rev. Mod. Phys. **83**, 349 (2011)
36. Ferrero, M., Parcollet, O.: TRIQS: a Toolbox for Research in Interacting Quantum Systems. http://ipht.cea.fr/triqs
37. Aichhorn, M., et al.: Phys. Rev. B **80**, 085101 (2009)
38. Boehnke, L., et al.: Phys. Rev. B **84**, 075145 (2011)
39. Skornyakov, S.L., et al.: Pis'ma v ZhETF **96**, 123 (2012). [JETP Letters **96**, 118 (2012)]
40. Ferber, J., et al.: Phys. Rev. B **85**, 094505 (2012)
41. Lee, G., et al.: Phys. Rev. Lett. **109**, 177001 (2012)
42. Vidberg, H.J., Serene, J.W.: J. Low Temp. Phys. **29**, 179 (1977)
43. Borisenko, S.V., et al.: Phys. Rev. Lett. **105**, 067002 (2010)
44. Yi, M., et al.: New J. Phys. **14**, 073019 (2012)
45. Cui, S.T., et al.: Phys. Rev. B **86**, 155143 (2012)
46. Fink, J., et al.: arXiv:1501.02135
47. Nekrasov, I.A., Pavlov, N.S., Sadovskii, M.V.: Pis'ma v ZhETF **95**, 659 (2012). [JETP Letters **95**, 581 (2012)]
48. Nekrasov, I.A., Pavlov, N.S., Sadovskii, M.V.: Zh. Eksp. Teor. Fiz. **143**, 713 (2013). [JETP **116**, 620 (2013)]
49. Nekrasov, I.A., Pavlov, N.S., Sadovskii, M.V.: Pis'ma. Zh. Eksp. Teor. Fiz. **97**, 18 (2013). [JETP Lett. **97**, 15 (2013)]
50. Nekrasov, I.A., Pavlov, N.S., Sadovskii, M.V.: Zh. Eksp. Teor. Fiz. **144**, 1061 (2013). [JETP **117**, 926 (2013)]
51. Brouet, V., et al.: Rev. B **86**, 075123 (2012)